A Refutation Of Special Relativity: II. Charge Particle Motion in Magnetic and Electric Fields

Eric Samuel (easamuel31415@gmail.com)
George Mason University

Physical Sciences - Article

Keywords: Radiation Damping Force, Synchrotron Radiation, Free Electron Lasers, Particle Accelerations

Posted Date: February 23rd, 2021

DOI: https://doi.org/10.21203/rs.3.rs-259013/v1

A Refutation Of Special Relativity:

II. Charge Particle Motion in Magnetic and Electric Fields

Eric A. Samuel

Abstract

Models for the radiation damping force of a charged particle in a magnetic or electric field by means of a flux-proportional Lentz force has been shown to be an elegant solution for the inward spiraling trajectories under magnetic fields, and the speed limited trajectories under electric fields. Our phenomenological formulation of the damping force in a magnetic field requires a new attenuation coefficient, α, that has only been evaluated using experimental data, but whose pure theoretical evaluation may lead to improved understanding of the mechanism of electron damping in electromagnetic fields. We believe that the synchrotron radiation and its observed coherence is already sufficient experimental evidence for our modeling of radiation damping. It is hoped that our model could be applied to improve the designs of free electron lasers as well as the design of particle accelerators.

Introduction

Newton's laws of motion (1) were universally accepted until the turn of the last century, when the Special Theory of Relativity (2) introduced the radical view that time, mass, and energy were dependent on the relative speed between frames of reference. The Special Theory of Relativity (SR) is universally accepted today despite its contravention of the principles of time and mass invariance that are axiomatically implicit in Newtonian theory. In the first installment of an intended series of papers (3), we provided rational arguments, and a proof, that the Special Theory of Relativity (SR) is fundamentally untenable, because the derivation of its core concept of time dilation is flawed by the expectation of inertial frame outcome for an unusual experimental design that isolates the observer and light clock apparatus in separate frames of reference with relative velocity. If the conclusions of our paper (3) are borne out, then time dilation and all its derivative concepts become unacceptable, and we will need to reset the framework of fundamental physics laws to restore the universality of Newtonian theory to the exclusion of SR.

In the forthcoming new installments of our paper series, we provide remarkable classical interpretations of the many brilliant experiments that have been narrowly extolled as supporting SR. This second paper proposes a new classical approach to explaining the motions of electron in magnetic and electric fields.

The turn of the last century also saw the innovation of clever experimental techniques (4 to 7) that sought to prove many of the predictions of SR. Most notable among these are the experiments of Guye and Levanchy that are currently upheld as providing one of the bast proofs of SR. The last mid century also saw the emergence of an astonishing new instrument, the bubble chamber (8, 9), that permitted the photographic capture of charged fundamental particles tracks including those electrons and mesons and their anti-particles. Finally, there has been a constant pedagogical effort, toward the end of the last century, to develop elegant yet simple beta spectrometers for student use to demonstrate and measure the velocities and kinetic energies of electrons exposed to magnetic fields (10 to 13). There has not been a strong effort to develop simple laboratory instruments for the experimental characterization of electrons exposed to electric fields. Bertozzi's (15) outstanding experiment remains the only source of kinetic data for electrons propelled by electric fields. Lund, M. and Uggerhøj (16) have developed a laboratory-intended technique for electrons in a magnetic field, but their interesting data for theory verification involves a linear accelerator whose geometrical and operational details are not provided in their paper.

This second paper is organized as follows: The Results section below has 2 major sections: (1) The motion of charged particles in a magnetic field, and (2) The motion of charged particles in an electric field. Each of these sections contains a theoretical part developing a phenomenological theory to explain the motions of charged particles in magnetic or electric fields, and an experimental part that applies the developed theory to explain experimental data and reflect on the lessons learned from the model-based comparison of experiment and theory.

Results

The motion of charged particles in a magnetic field

It is well known that the trajectories of electrons, positrons and other charged particles are inward looping spirals. The 4 insets in Figure 1 are selected examples of bubble chamber tracks of electrons and positrons in magnetic fields (4, 5). In the absence of electron energy loss, Lawrence (14) showed that the electron trajectory in an H-field is theoretically an overlapping circle. Although it is generally acknowledged in the literature that the inward spiral tracks are due to energy loss by radiation and by collisions, no theoretical model for such a spiral track has yet been developed. Figure 1 reveals an astonishing fact; even though the tracks are drawn from different events and possibly different bubble chambers, they can all be mathematically interpreted in terms of the simple polar equation for a spiral:

$$r = r_0 e^{-\alpha\theta} \qquad -(1)-$$

$$ln(r) = ln\,(r_0) - \alpha\theta \qquad -(2)-$$

In Equations (1) and (2), r and $r_0$can be in arbitrary but consistent units, and the polar angle θ is in radians. The data displayed in Figure 1 was digitized by uploading the track snippet into Matlab[R] and using the *ginput* command to obtain the track's radial

Figure 1

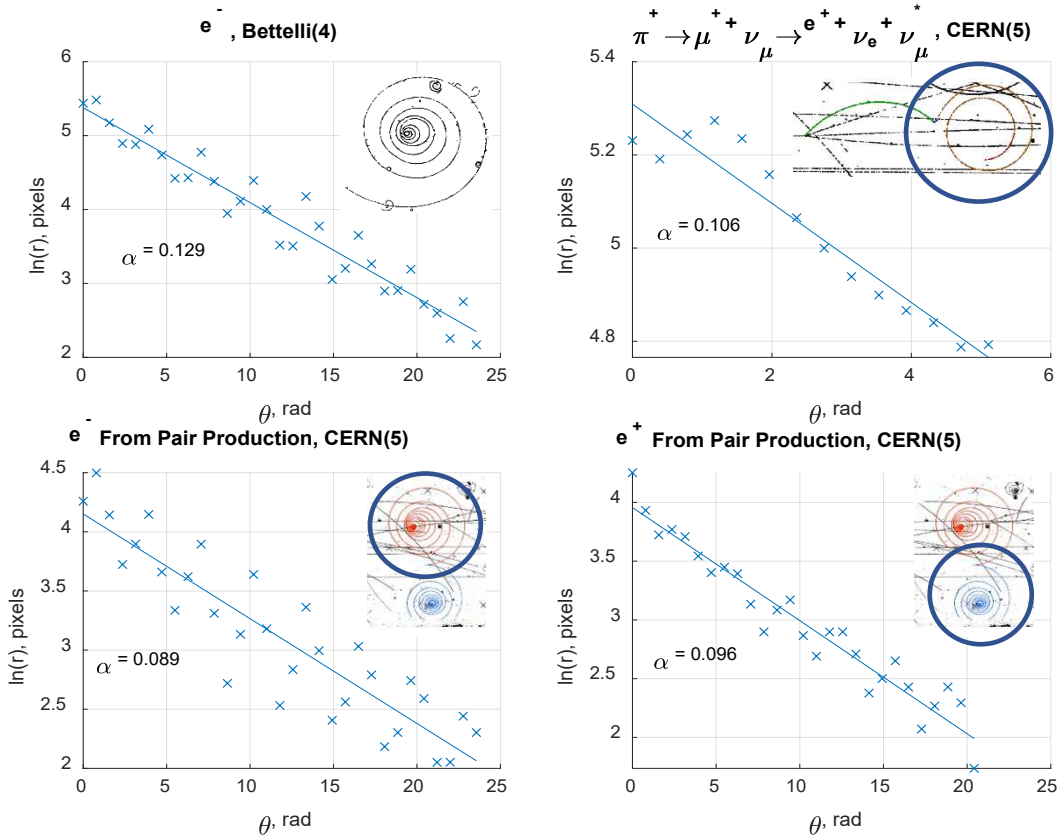

Select bubble chamber tracks fitted to the simple spiral equation (1), above.

position, expressed in pixels, incrementally at every π/2 of its angular position in the track. Since the angular positions are preserved in photographic magnifications, the attenuation factor, α, is preserved through the magnifications and the magnification scale factor is absorbed into r_0. For the tracks in Figure 1, α is in the range of 0.089 to 0.129. Equation (1) thus places a constraint on any theory for a charged particle track in an H-field.

Our phenomenological theory for the motions of charged particles in magnetic fields is based on modeling the radiative energy loss of a particle as a force conforming to Lenz's law. The total force on the charged particle in a magnetic field, $\vec{\boldsymbol{B}}$, is then a modification of the Lorentz motive force by adding the Lentz retarding force:

$$F_H = m_e\vec{\boldsymbol{a}} = \; e\,\vec{\boldsymbol{v}}\,\mathrm{x}\,\vec{\boldsymbol{B}} - \alpha\, e\frac{\vec{\boldsymbol{B}}\; x\;\vec{\boldsymbol{v}}\,\mathrm{x}\,\vec{\boldsymbol{B}}}{\left|\vec{\boldsymbol{B}}\right|} \qquad -(3)-$$

where e is the signed charge of the electron, m_e its mass, and α the phenomenological attenuation coefficient of Equations (1) and (2), and of Figure (1). The vector formulation and sign of the attenuation term in Equation (3) will assure that the attenuating force is in a direction opposing the forward velocity vector, $\vec{\boldsymbol{v}}$.

Equation (3) can be decomposed into normal and tangential components:

$$m_e\frac{v^2}{r} = evB \qquad -(3a, Normal\ Component)-$$

$$\omega = \frac{eB}{m_e} \qquad -(3b)-$$

As shown by Lawrence (14), the normal component of Equation (3) results in an angular velocity, ω, that remains constant throughout the track's lifetime despite its loss of tangential velocity. The constant, ω, certainly simplifies the solution of tangential component of Equation (3):

$$m_e\dot{v} = \; -\alpha\, eBv \qquad -(4a, Tangential\ Component)-$$

$$\dot{v} = \; -\alpha\,\omega\, v \qquad -(4b)-$$

$$\frac{dv}{v} = \; -\alpha\,\omega\, dt \qquad -(4c)-$$

The simple solution to Equation (4c) is:

$$v = \; v_0 e^{-\alpha\omega t} \qquad -(4d)-$$

where v_0 is the track's tangential speed at time t=0. Equation (4d) can be reduced to the form of Equation (1) by observing 2 definitions:

$$\theta = \omega t \;\; and\; \omega = \frac{v}{r} \qquad -(4e)-$$

where $r(t)$ and $\theta(t)$ are the track's polar coordinates. Using both definitions of Equation (4e), the final simplifications of the track are:

$$v = \; v_0 e^{-\alpha\theta} \qquad -(4f)-$$

$$r = \; r_0 e^{-\alpha\theta} \qquad -(4g)-$$

Equation (4g) for the spiraling of the radial component follows from the constancy of the angular velocity, and the second of Equations (4e). Since Equation (4e) is identical to Equation (1), the simple Lentz formulation for the retarding force on the

charged particle permits the derivation for the simple track trajectory that is amenable to fitting the experimental track data.

We now turn to comparing the experimental data from a select number of laboratory β-spectrometers with our theoretical spiral trajectories. Our selection of spectrometers (9 to 13) is based on considerations of simplicity of design, testing and calibration procedures, and potential accuracy of the measurements. Previous, SR-centric interpretations of the data from the selected spectrometers are not admissible because

Figure 2

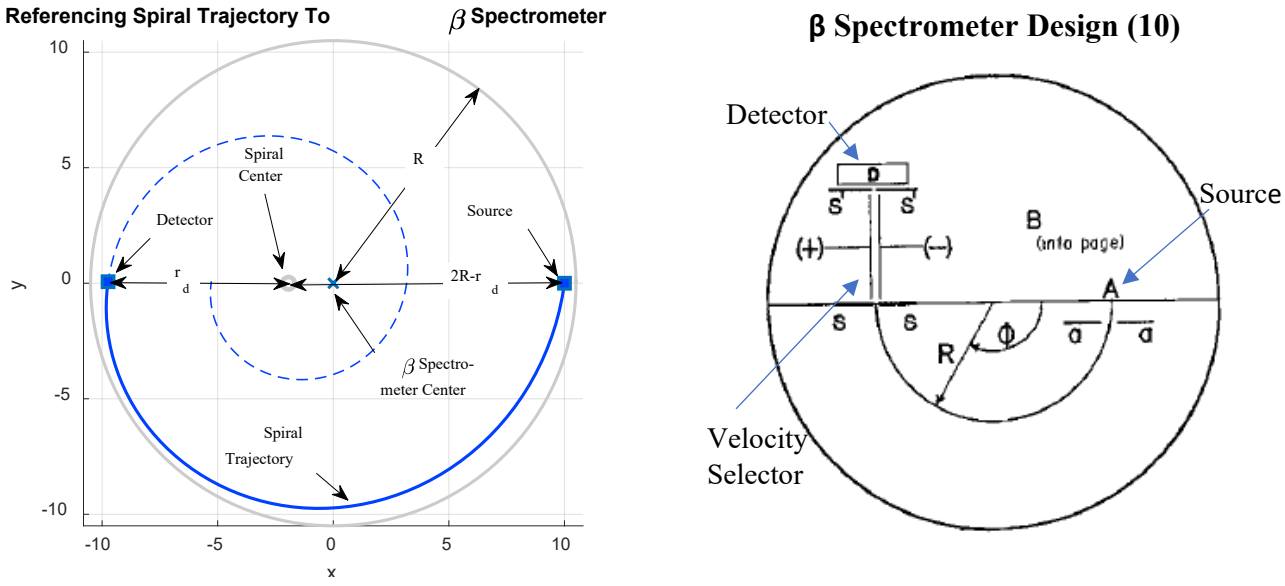

Left panel: Referencing spiral trajectory to β spectrometer.
Right panel: β spectrometer components

of their contrived circular trajectory fits that contradict the vast evidence for spiral trajectories (as discussed above). Figure 2 shows how the spiral trajectories reference center is displaced with respect to the geometric center of the spectrometer. Figure 2

also shows a typical spectrometer design and its main components. The Bartlett and Correl (10) uses a Bucherer-style velocity selector in front of its detector, while the remaining designs some use the spectrometer's magnetic field as the velocity selector together with calibrated kinetic energy detectors.

Our procedure to fit the spectrometer data to the theoretical trajectory of Equation (1) is as follows:

1. Calculate the operating value of the trajectories angular velocity, ω, from the operating value of the magnetic field.
2. Deduce the final electron speed (v_f) from the measured kinetic energy. Bartlett and Correl (10) report v_f directly.
3. Apply the 2nd of Equation (4e) to obtain the distance, $r_d = \frac{v_f}{\omega}$.
4. Impose the condition that ω is constant to determine the perpendicular distance of the initial (source) velocity vector to the center of the spiral trajectory, $= (2R - r_d)$ as shown in Figure 2.
5. Calculate α using Equation (2) for a final angular position of $\theta = \pi$, as:

$$\alpha = -\frac{\ln\left(\frac{r_d}{2R - r_d}\right)}{\theta} \qquad -(5)-$$

Figure (3) summarizes the attenuation coefficients, α, obtained as outlined above, from all 4 data sets.

Figure 3

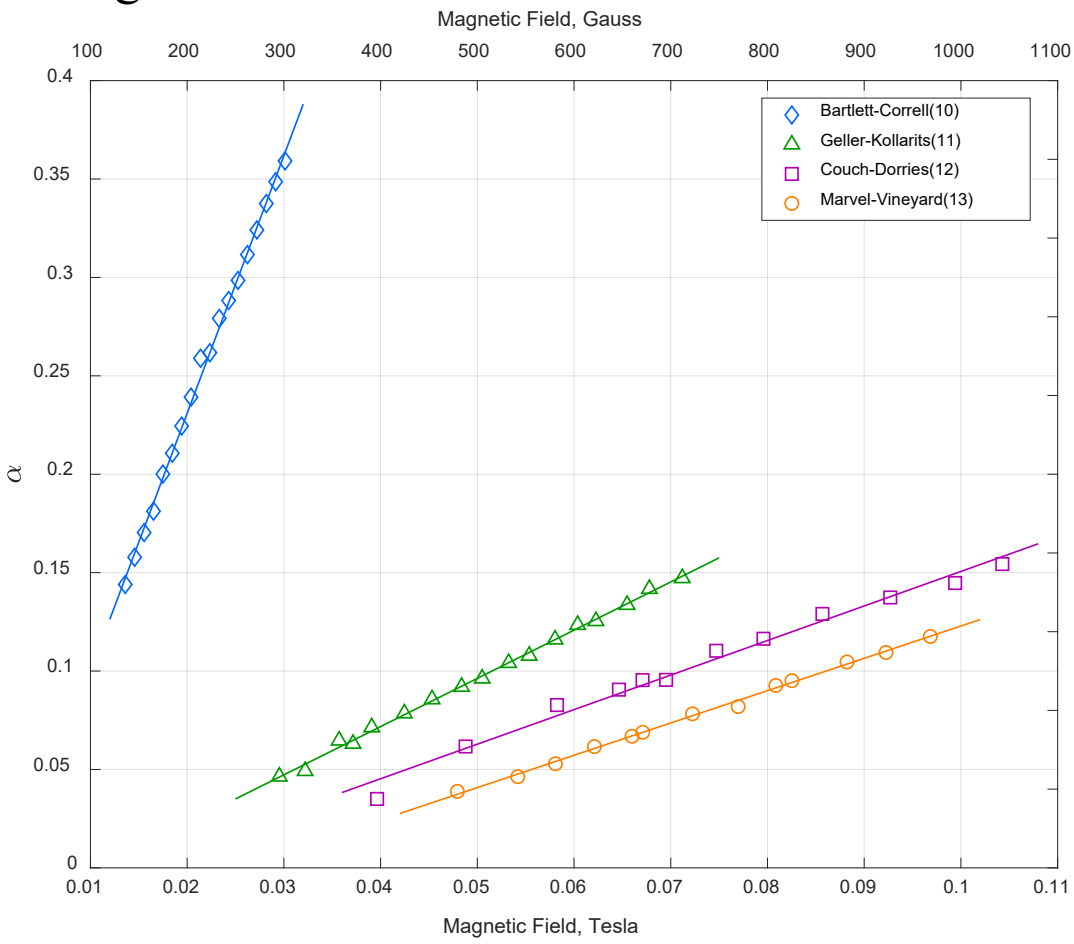

Radiation damping attenuation constants for electrons in a magnetic field from spectrometer measurements.

The following characteristics of the α values are evident:

1. α appears to be dependent linearly on the magnetic field
2. The Bartlett and Correll (10) data show alfa values significantly larger than the remaining 3 data sets that are roughly grouped together.
3. The appears to be significant experimental error in determining α as judged from their significant deviations among data sets.
4. Except 3 data sets that are roughly grouped together appear to agree reasonable with the previously discussed α values from bubble chamber trajectories.

The above behaviors can be valuable in further refinements of the spectrometer experiments, and further theoretical developments for closely understanding the radiation-induces damping constant, α.

The motion of charged particles in an electric field

SR's universal speed limit, nor the mass increase with electron speed can no longer be used to understand Bertozzi's classical experiment (15), since we believe that SR's theoretical basis is tenuous, and because the radiation damping of the electron trajectories in an electric field have not been hitherto considered. In the case of an electro in a magnetic field, we found its inward spiral trajectory to be the key to modeling the radiation damping force above. In the case of an electro in an electric field, the key is the limiting speed observed by Bertozzi. In this case, a radiation damping formulation emerges when an analogy is drawn between the damped electron motion in an electric field to a falling rain droplet speed limited under Stokes drag. Since the net force on the electron is zero at its terminal speed of c, the augmented Lorentz force with a flux-proportional Lentz force is:

$$F_E = m_e\vec{\boldsymbol{a}} = \; e\,\vec{\boldsymbol{E}} - \frac{e}{c}\,\vec{\boldsymbol{v}}\cdot\vec{\boldsymbol{E}} \qquad -(6)-$$

When applied to the Bertozzi experiment, Equation (6) becomes:

$$m_e\dot{v} = \; e\,E - e\frac{v}{c}\,E \qquad -(7)-$$

Equations (6) and (7) satisfy the requirement for net force on the electron to be zero at its terminal speed of c. The solution to Equation (7) for an initial zero electron velocity, is:

$$\beta = \frac{v}{c} = c\left(1 - e^{-\frac{t}{\tau}}\right), \tau = \frac{c\, m_e}{eE}\ , E = \frac{V}{d} \qquad -(8a)-$$

$$x = \int_0^t v(t)dt = c\, t - c\tau\left(1 - e^{-\frac{t}{\tau}}\right) = c\, t - v\tau \qquad -(8b)-$$

Equations (8a) and (8b) are directly applicable to Bertozzi's first 3 data points obtained with only the van De Graff generator activated and the Linac disabled. Under the above controlled conditions, we first apply Equation 8(a) to obtain the time of flight for an assumed Van de Graff chamber length, d, and then calculate a distance travelled, x, for that time of flight. This calculated should be theoretically equal to d the assumed Van de Graff chamber length.

Figure 4 shows the variation of the electron speed and its traversed distance. The assymptotic straight lines of equal slope and intercepts varying with electric field are

Figure 4

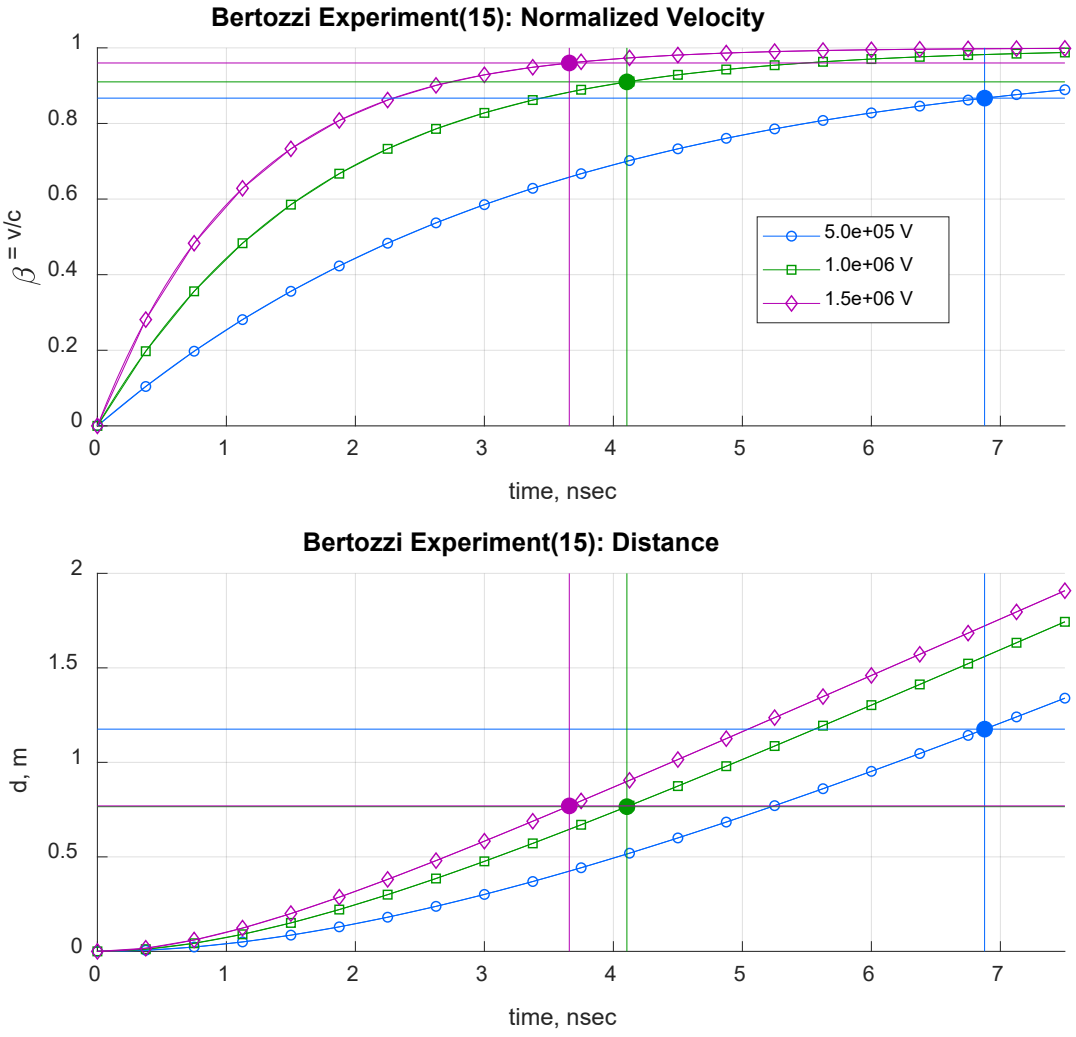

Bertozzi data compared with theoretical predictions for electron velocity and position.

evident in Figure 4's lower panel. The 3 experimental points form Bertozzi are also marked on the plots. Table 1 summarizes the comparison further.

Table 1

Theoretical predictions for Betozzi's (15) first 3 experimental data points

V, MV	Assumed, d, m	E, V/m	β = v/c	t, ns	x(t), m	Error, x-d, m
0.50	1.00	5.00E+05	0.87	6.88	1.18	0.18
1.00	1.00	1.00E+06	0.91	4.11	0.77	-0.23
1.50	1.00	1.50E+06	0.96	3.66	0.77	-0.23
				Avg	0.90	

The theoretical predictions for the Bertozzi data are reasonable, given that the operational length, d, of the van De Graff tube was not disclosed in the paper.

Discussion

We have shown that modeling the radiation damping force of a charged particle in a magnetic or electric field by means of a flux-proportional Lentz force leads to an elegant solution for the inward spiraling trajectories under magnetic fields, and the speed limited trajectories under electric fields. However, in the case of the magnetic field-influenced trajectories, the phenomenological formulation of the damping force creates a new attenuation coefficient, α, that has only been evaluated using experimental data, but whose pure theoretical evaluation may lead to improved understanding of the mechanism of electron damping in electromagnetic fields. We believe that the synchrotron radiation and its observed coherence is already sufficient experimental evidence for our modeling of radiation damping. It is hoped that our model could be applied to improve the designs of free electron lasers. The design of particle accelerators certainly should factor in the damping force modelled here.

References

1. Newton, I. Philosophiae Naturalis Principia Mathematica, Streater, London (1687) Newton, I. Principles of Natural Philosophy, Univ of California Press, Berkeley, (1934); paperback, (1962)

2. Einstein, A. Zur Elektrodynamik bewegter Körper, *Ann. Physik* 17, 891 (1905)

3. Samuel, E. A., A Refutation Of Special Relativity: I. Disproving Time Dilation, submitted to *Nature* (2021).

4. Kaufmann, W., Die elektromagnetische Masse des Elektrons (The Electromagnetic Mass of the Electron), *Physikalische Zeitschrift*, 4 (1b), 54–56 (1902)

5. Bucherer, A. H., Die experimentelle Bestätigung des Relativitätsprinzips, *Ann. Physik* 333(3), 513 (1909)

6. Neumann, G., Die träge Masse schnell bewegter Elektronen, *Ann Physik* 350 (20): 529–579 (1914)

7. Guye, C.E. and Lavanchy, C., Vérification expérimentale de la formule de Lorentz–Einstein par les rayons cathodiques de grande Vitesse, *Comptes Rendus* 161: 52–55(1915)

8. Bettelli, L., Bianchi-Streit, M. and Giacomelli, G., Particle Physics With Bubble Chamber Photographs, Fermilab archive: https://lss.fnal.gov/archive/other/print-93-0553.pdf

9. CERN educational website: https://scool.web.cern.ch/sites/scool.web.cern.ch/files/documents/20180811_JW_Student_worksheet_solutions_Bubble_%20chamber_pictures.pdf

10. Bartlett, A. and Correll, M. An Undergraduate Laboratory Apparatus for Measuring as a Function of Velocity. I, *Am. J. Phys.* 33, 327 (1965)

11. Geller. K.N. and Kollarits, R., Experiment to Measure the Increase in Electron Mass with Velocity, *Am. J. Phys.* 40, 1125 (1972)

12. Couch, J. G. and Dorries, T.K. Measuring relativistic electrons in the undergraduate laboratory, *Am. J. Phys*. 50, 917 (1982)

13. Marvel, R. E. and Vineyard, M. F., Relativistic Electron Experiment for the Undergraduate Laboratory, arXiv:1108.5977v1, (2011)

14. Lawrence, E. O. and Livingston, M. S. , The Production of High Speed Light Ions Without the Use of High Voltages, *Phys. Rev.* 40 (1): 19–35 (1932)

15. Bertozzi, W., Speed and Kinetic Energy of Relativistic Electrons, *Am. J. Phys*. 32, 551 (1964), *Am. J. Phys*. 32, 551 (1964)

16. Lund, M. and Uggerhøj, U. I. Experimental special relativity with a meter stick and a clock, *Am. J. Phys*. 77, 757 (2009)

Acknowledgements

This work was completed without external support.

Author Information

Affiliations

Dept. Of Mechanical Engineering, George Mason University, Fairfax, VA 22030, USA

Contributions

Author contributed entirely to all aspects of this work.

Corresponding author

Correspondence to E. Samuel by email only, email address: easamuel31415@gmail.com

Ethics Declaration

Competing interests

The author declares no competing financial interests.

Figures

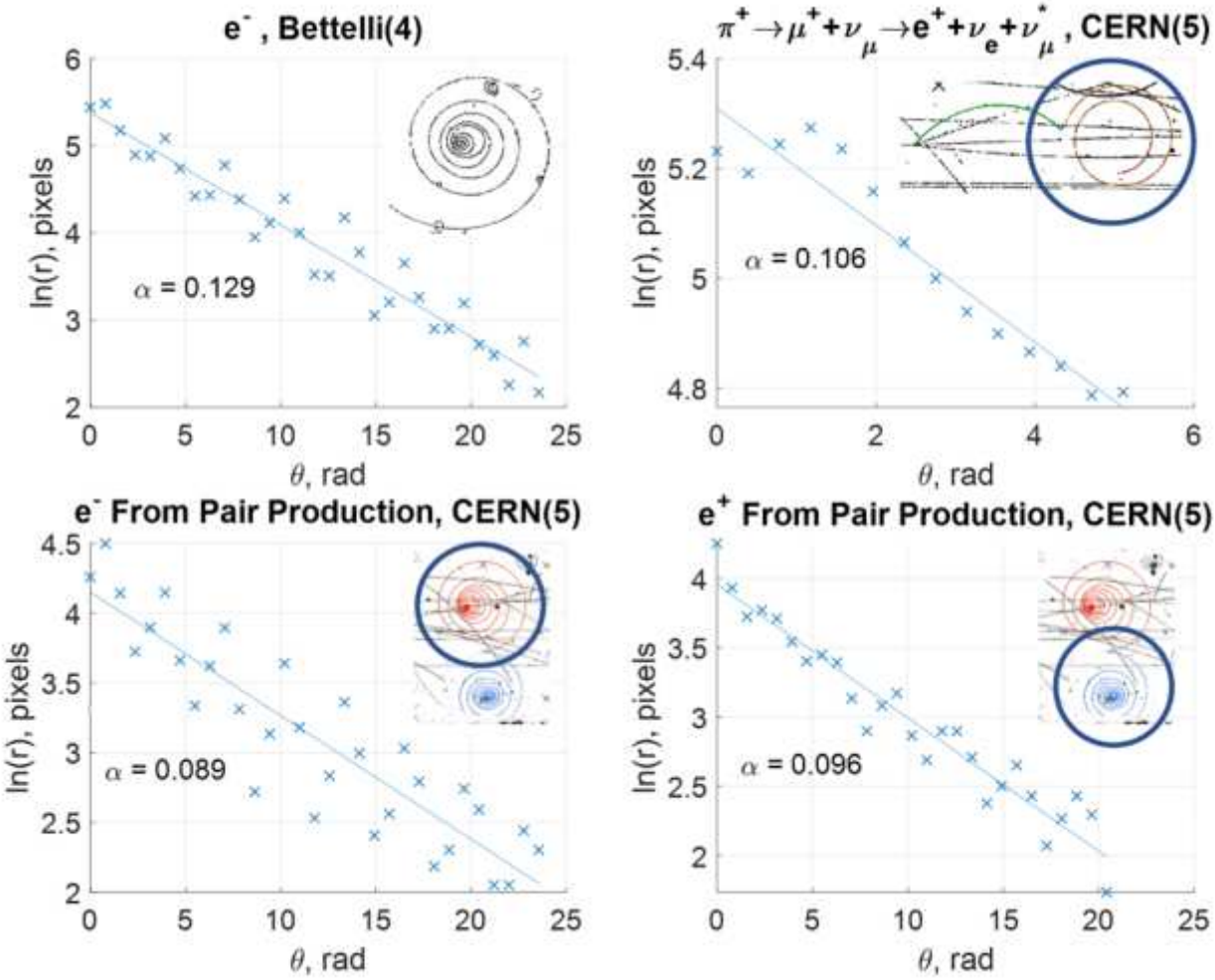

Figure 1

Select bubble chamber tracks fitted to the simple spiral equation (1), above.

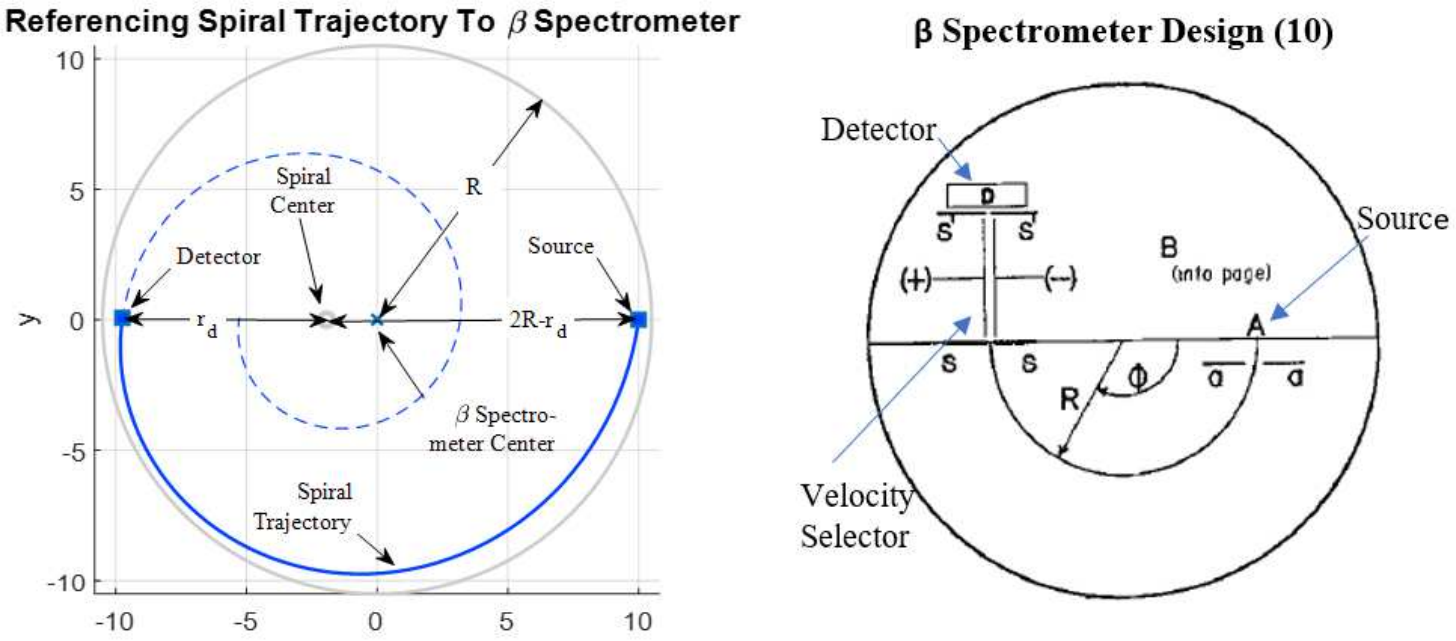

Figure 2

Left panel: Referencing spiral trajectory to β spectrometer. Right panel: β spectrometer components

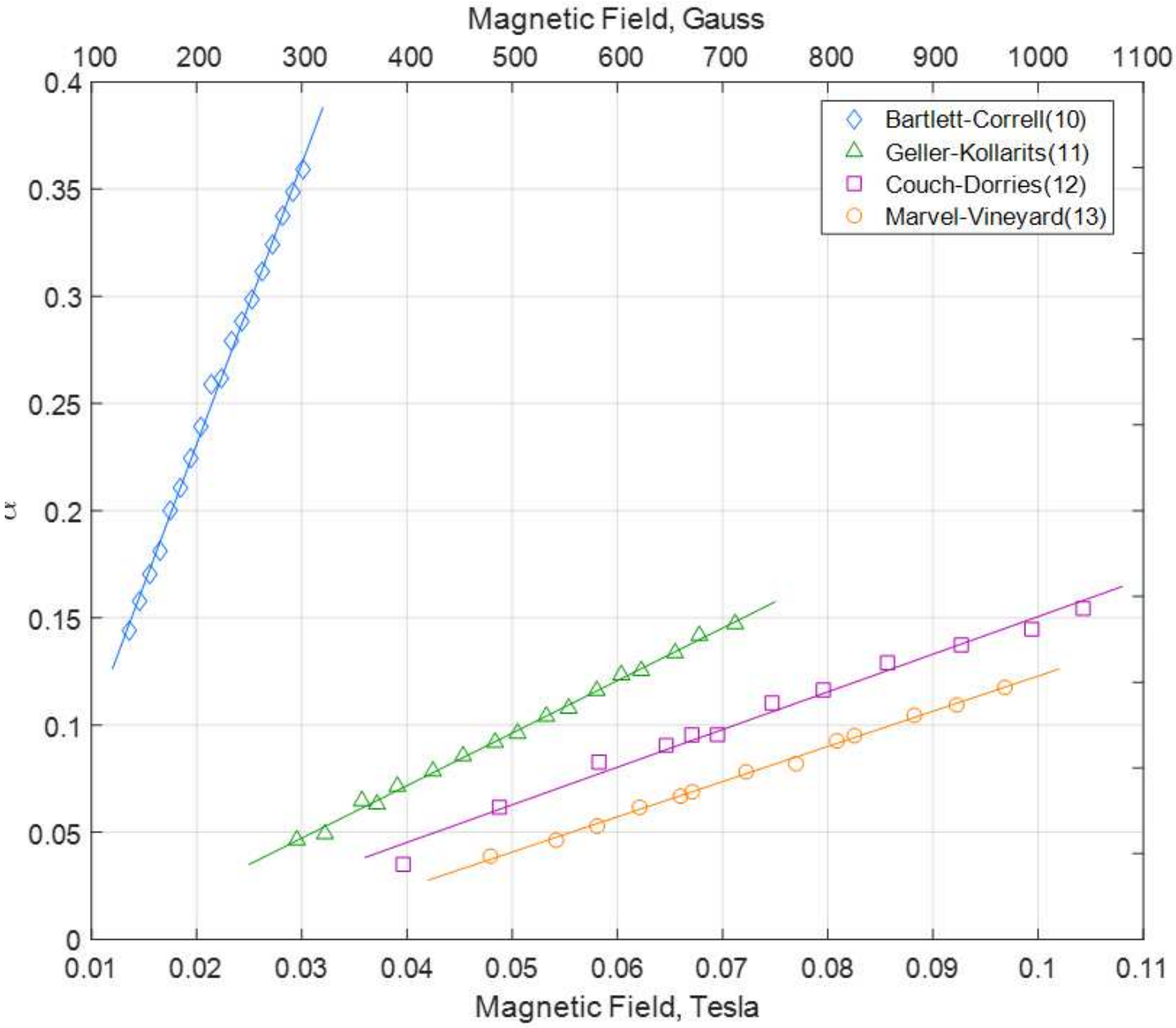

Figure 3

Radiation damping attenuation constants for electrons in a magnetic field from spectrometer measurements.

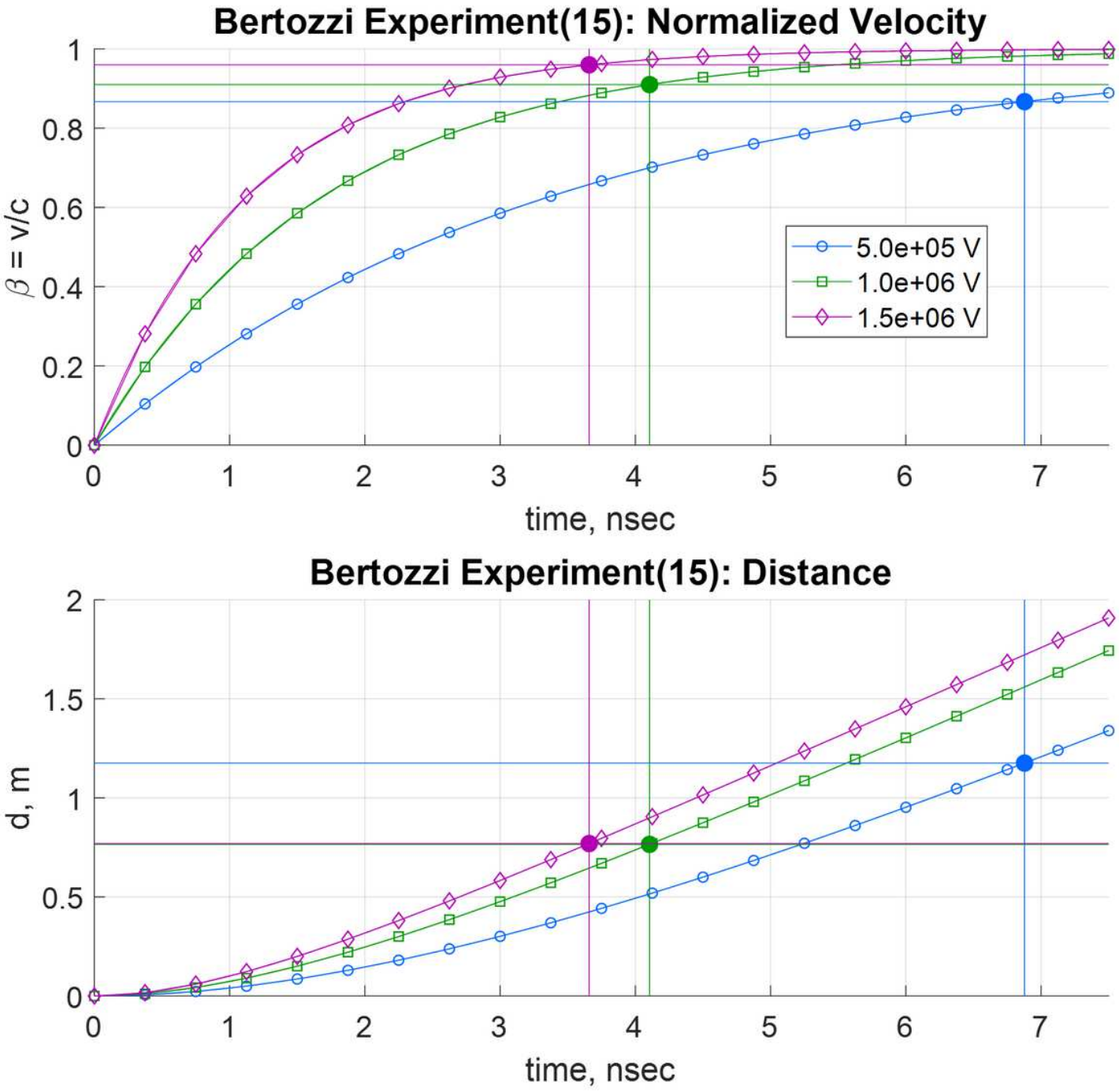

Figure 4

Bertozzi data compared with theoretical predictions for electron velocity and position.